4420 *Inorg. Chem.* **2010**, *49*, 4420–4432
DOI: 10.1021/ic100034q

Inorganic Chemistry
Article

Structural Study of the *N,N'*-Dimethylpropyleneurea Solvated Lanthanoid(III) Ions in Solution and Solid State with an Analysis of the Ionic Radii of Lanthanoid(III) Ions

Daniel Lundberg,*,[†] Ingmar Persson,*,[†] Lars Eriksson,[‡] Paola D'Angelo,[§] and Simone De Panfilis[||]

[†]*Department of Chemistry, Swedish University of Agricultural Sciences, P.O. Box 7015, SE-750 07 Uppsala, Sweden,* [‡]*Department of Chemistry, Division of Structural Chemistry, Arrhenius Laboratory, Stockholm University, SE-106 91 Stockholm, Sweden,* [§]*Department of Chemistry, University of Rome "La Sapienza", Piazzale Aldo Moro 5, I-00185 Rome, Italy, and* [||]*European Synchrotron Radiation Facility, B.P. 220, F-38043 Grenoble Cedex, France*

Received September 6, 2009

The structures of the *N,N'*-dimethylpropyleneurea (dmpu) solvated lanthanoid(III) ions have been studied in dmpu solution (La−Nd, Sm−Lu) and in solid iodide salts (La−Nd, Sm, Gd−Lu) by extended X-ray absorption fine structure (EXAFS), and single crystal X-ray diffraction (La, Pr, Nd, Gd, Tb, Er, Yb, and Lu); the EXAFS studies were performed on both K and L_{III} absorption edges. Because of the space-demanding properties of dmpu upon coordination, dmpu solvated metal ions often show coordination numbers lower than those found in corresponding hydrates and solvates of oxygen donor solvents without steric requirements beyond the size of the donor atom. All lanthanoid(III) ions are seven-coordinate in solution, except lutetium(III) which is six-coordinated in regular octahedral fashion, whereas in the solid iodide salts the dmpu solvated lanthanoid(III) ions are all six-coordinate in regular octahedral fashion. A comparison of Ln−O bond lengths in a large number of lanthanoid(III) complexes with neutral oxygen donor ligands and different configurations shows that the metal ion-oxygen distance is specific for each coordination number with a narrow bond distance distribution. This also shows that the radius of the coordinated oxygen atom in these compounds can be assumed to be 1.34 Å as proposed for coordinated water, while for ethers such as tetrahydrofuran (thf) it is somewhat larger. Using this atomic radius of oxygen in coordinated water molecules, we have calculated the ionic radii of the lanthanoid(III) ions in four- to nine-coordination and evaluated using the bond lengths reported for homo- and heteroleptic complexes in oxygen donor solvates in solution and solid state. This yields new and revised ionic radii which in some instances are significantly different from the ionic radii normally referenced in the literature, including interpolated values for the elusive promethium(III) ion.

Introduction

The coordination chemistry of the lanthanoid(III) ions follows a more regular pattern than any other series in the periodic table because of the identical outer shell electron configuration, $5s^25p^6$, of 15 elements in a row, $Z = 57-71$.[1] This makes the elements in the lanthanoid series notoriously hard to chemically separate from each other,[2] but ideal for comparative studies in coordination chemistry. The triply charged lanthanoid ions have typical hard Lewis acid binding properties, forming mainly electrostatic interactions, which, in turn, cause the coordination number (CN) to be largely limited by geometric restrictions.[3] If the lanthanoid(III) ions were to coordinate to oxide or oxygen donor ligands from a strictly geometric point-of-view eight-coordination is a good approximation for the entire series.[4,5] Applying the hard and soft acids and bases (HSAB) theory does not change this fact,[3] as the radius ratio between the metal ion and the donor ligand atom still is governed by the same set of geometric rules, see Table 1. Because of stabilization effects arising from extensive hydrogen bonding networks this value can be increased, as seen in the structures of the hydrated lanthanoid(III) ions, that are nine-coordinate in a trigonal tricapped (*ttp*) configuration throughout the series for the trifluoromethanesulfonate salts,[6−9] even though the heavier lanthanoid(III) ions display some water deficiency in the

---

*To whom correspondence should be addressed. E-mail: daniel.lundberg@kemi.slu.se (D.L.), ingmar.persson@kemi.slu.se (I.P.). Fax: (+46) 18-673476.

(1) Shannon, R. D. *Acta Crystallogr., Sect. A* **1976**, *32*, 751–767.

(2) For a complete listing of historical references, see Supporting Information, Table S1.

(3) Pearson, R. G. *J. Am. Chem. Soc.* **1963**, *85*, 3533–3539.

(4) Pauling, L. *J. Am. Chem. Soc.* **1927**, *49*, 765–790.

(5) Pauling, L. *J. Am. Chem. Soc.* **1929**, *51*, 1010–1026.

(6) D'Angelo, P.; Zitolo, A.; Migliorati, V.; Mancini, G.; Persson, I.; Chillemi, G. *Inorg. Chem.* **2009**, *48*, 10239–10248.

(7) Persson, I.; D'Angelo, P.; De Panfilis, S.; Sandström, M.; Eriksson, L. *Chem.*—*Eur. J.* **2008**, *14*, 3056–3066.

(8) Allen, F. H. *Acta Crystallogr., Sect. B* **2002**, *58*, 380–388.

(9) *Inorganic Crystal Structure Database 1.4.6* (release: 2009−2); FIZ/NIST: Karlsruhe, Germany.

Table 1. Limiting Radius Ratios (Central Ion/Coordinating Atom), ρ, for the Most Commonly Found Geometric Configurations and CNs[a]

ρ	configuration	CN
<0.155	linear	2
0.155	trigonal	3
0.225	tetrahedral, T_d	4
0.414	square planar, *sqpl*	4
0.414	trigonal bipyramidal, *tbp*	5
0.414	square pyramidal, *sapy*	5
0.414	octahedral, O_h	6
0.645	square antiprismatic, *sap*	8
0.732	cubic	8
0.732	tricapped trigonal prismatic, *ttp*	9
>1.000	cuboctahedral	12

[a] Adapted from refs 3−5.

capping positions.[6,10−12] EXAFS and XANES (X-ray absorption near edge structure) studies have shown that the coordination geometry of the hydrated lanthanoid(III) ions present in the hydrated trifluoromethanesulfonate salts is maintained in aqueous solution.[7,10,11] The dimethylsulfoxide (dmso) solvated lanthanoid(III) ions have all been found to be eight-coordinate in square antiprismatic (*sap*) fashion in the solid iodide salts and in dmso solution,[13,14] as well as a vast majority of the lanthanoid(III) complexes and compounds with oxygen donor ligands.[8,9] This is expected from a geometrical point-of-view, where comparisons between solution and solid state are imperative to avoid misinterpretation of individual data sets.[15−17]

Lower CNs (CN < 8) are not unheard of, but are rare in comparison to the higher ones, and usually involve large ligands that prohibit normal coordination behavior. There are, however, ligands such as Keggin or Keggin-like structures that sometimes are referred to as bulky polydentate ligands that still exhibit high CNs, thereby urging for a more precise definition of sterical demands.[18] Other ligands can be classified as space-demanding *upon coordination*, as they, beside the limited radius ratio of their donor atom, have specific structural features with spatial requirements close to the donor atom which may cause a reduction in the CN for the metal ion without being large or bulky in the traditional sense. Hexamethylphosphoric amide (hmpa)[19−22] and substituted ureas like tetramethylurea (tmu),[23−27] are prime examples, as their respective *N*-methyl groups are sufficiently close to the electron pair donating oxygen atom to have a significant effect on the space required upon coordination, and thereby on the available upper CN. The actual spatial requirements of such ligands, for example, in terms of cone angle, are yet to be quantified as Tolman did for *P*-donor ones,[28] but it lies out of the scope of this article. Another requirement for determination of the spatial demands of a ligand is the use of coordinating metal ions with a fair degree of hardness, as soft metal ions may opt for lower CNs than geometrically feasible because of their electronic properties.[29,30]

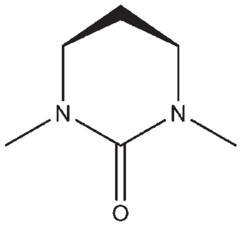

Figure 1. Structure formula of the essentially flat *N,N*′-dimethylpropyleneurea, dmpu, where the middle propylene carbon atom lies out of the plane. The methyl groups bordering the coordinating oxygen make the ligand space-demanding upon coordination. For purposes of clarity, hydrogens have been omitted.

It is important to stress that space-demanding ligands do not alter the intrinsic chemical properties of the coordinating atom in the ligand, which allows for comparison between different complexes with the same donor atom with less or no coordination-related steric requirements. The study of solvent molecules that are space-demanding upon coordination is consequently worth extra attention, as this often gives insights into the physicochemical properties and behavior of metal ions not found in aqueous solution and in other solvents with common CNs and configurations;[19−27,31,32] for example, it has been shown that the complex formation is much stronger (i.e., increased reactivity) in solvents where the solvated metal ion is five-coordinate than in solvents where it is octahedrally solvated.[31,32]

In the present study, the solvent ligand *N,N*′-dimethylpropyleneurea (dmpu; IUPAC name: 3,4,5,6-tetrahydro-1,3-dimethyl-2(1*H*)-pyrimidinone; Figure 1) which is space-demanding upon coordination has been used to unveil possible changes in the coordination chemistry of solvated lanthanoid(III) ions, and to study complexes of lanthanoid(III) ions with lower CNs, in a systematic way. The two methyl groups bordering the electron-pair donating oxygen and the semirigid ring structure have been shown to obstruct the common coordination, forming metal ion solvates with

---

(10) Abbasi, A.; Lindqvist-Reis, P.; Eriksson, L.; Sandström, D.; Lidin, S.; Persson, I.; Sandström, M. *Chem.—Eur. J.* **2005**, *11*, 4065–4077.

(11) D'Angelo, P.; Zitolo, A.; Migliorati, V.; Persson, I. *Chem.—Eur. J.* **2010**, *16*, 684–692.

(12) Lindqvist-Reis, P.; Persson, I.; Sandström, M. *Dalton Trans.* **2006**, 3868–3878.

(13) Abbasi, A.; Damian Risberg, E.; Eriksson, L.; Mink, J.; Persson, I.; Sandström, M.; Sidorov, Y.; Skripkin, M.; Ullström, A. *Inorg. Chem.* **2007**, *46*, 7731–7741.

(14) Persson, I.; Damian Risberg, E.; D'Angelo, P.; De Panfilis, S.; Sandström, M.; Abbasi, A. *Inorg. Chem.* **2007**, *46*, 7742–7748.

(15) Ishiguro, S.; Kato, K.; Takahashi, R.; Nakasone, S. *Rare Earths* **1995**, *27*, 61–77.

(16) Ishiguro, S.; Kato, K.; Nakasone, S.; Takahashi, R.; Ozutsumi, K. *J. Chem. Soc., Faraday Trans.* **1996**, *92*, 1869–1875.

(17) Ishiguro, S.; Umebayashi, Y.; Kato, K.; Nakasone, S.; Takahashi, R. *Phys. Chem. Chem. Phys.* **1999**, *1*, 2725–2732.

(18) Niu, J.; Wei, M.; Wang, J. *J. Mol. Struct.* **2004**, *689*, 147–152.

(19) Huang, Q.; Wu, X.; Wang, Q.; Sheng, T.; Lu, J. *Angew. Chem., Int. Ed.* **1996**, *35*, 868–870.

(20) Barr, D.; Clegg, W.; Mulvey, R.; Snaith, R. *J. Chem. Soc., Chem. Commun.* **1984**, 226–227.

(21) Teng, W.; Englich, U.; Ruhlandt-Senge, K. *Angew. Chem., Int. Ed.* **2003**, *42*, 3661–3664.

(22) Gałdecka, E.; Gałdecki, Z.; Huskowska, E.; Amirkhanov, V.; Legendziewicz, J. *J. Alloys Compd.* **1997**, *257*, 182–190.

(23) Tanada, K.; Hashimoto, A.; Tsuji, H.; Kato, K.; Inada, Y.; Aizawa, S.; Funahashi, S. *Inorg. Chim. Acta* **2006**, *359*, 511–518.

(24) Aslanov, L.; Ionov, V.; Sotman, S. *Kristallografiya* **1976**, *21*, 1200–1201.

(25) Ng, S.; Hu, S. *Acta Phys.-Chim. Sin.* **2000**, *16*, 804–809.

(26) Lyubeznova, T.; Ponomaryev, V.; Aslanov, L. *Kristallografiya* **1990**, *35*, 746–750.

(27) Melo, S.; Jatahy, L.; Castellano, E.; Santos, C. *Inorg. Chim. Acta* **1985**, *109*, 163–166.

(28) Tolman, C. *Chem. Rev.* **1977**, *77*, 313–348.

(29) Persson, I.; Nilsson, K. B. *Inorg. Chem.* **2006**, *45*, 7428–7434.

(30) Nilsson, K. B.; Persson, I.; Kessler, V. G. *Inorg. Chem.* **2006**, *45*, 6912–6921.

(31) Bobicz, D.; Kristiansson, O.; Persson, I. *J. Chem. Soc., Dalton Trans.* **2002**, 4201–4205.

(32) Lundberg, D.; Ullström, A.; D'Angelo, P.; Warmińska, D.; Persson, I. *Inorg. Chim. Acta* **2007**, *360*, 2744–2750.

lower CNs than observed in the corresponding hydrates and dmso solvates. Such changes have been observed for iron(II),[33] iron(III),[33] nickel(II),[31] and zinc(II),[34] which are all five-coordinate in dmpu solution, while all these ions are six-coordinate in octahedral fashion in water, dimethyl sulfoxide (dmso), and *N*,*N*-dimethylformamide (dmf).[8,9,35] First manufactured as a replacement for the carcinogenic hmpa, dmpu is a polar, aprotic solvent with high donor strength ($D_S = 34$), high permittivity ($\varepsilon = 36.1$), large dipole moment ($\mu = 4.23$ D), and wide liquid range (249.4−519.7 K), used in an extensive array of applications.[36−42]

This study aims at exploring the coordination chemistry of dmpu solvated lanthanoid(III) ions in solution and solid state by EXAFS at both K and L_{III} edges, and by single crystal X-ray crystallography. This systematic study allowed us to compare not only solution and solid state structures, but also crystallographic and EXAFS results. This study concludes a wider investigation of the coordination chemistry of solvated lanthanoid(III) ions, previously covering the hydrates (CN $\approx$ 9)[6,7,10,11] and the dmso solvates (CN = 8).[13,14] Here we investigate a solvent which is space-demanding upon coordination, thus forcing the CN to be lower than both the hydrates, which have an extensive hydrogen bonding network thereby increasing the CN, and the dmso solvates with the geometrically expected CN.

In addition, the ionic radii of the lanthanoid(III) ions have been calculated and evaluated by summarizing the bond distances in reported structures of solvates in the solid state and solution of homoleptic and heteroleptic complexes with monodentate oxygen donor ligands. When one seeks to evaluate the ionic radii of metal ions it is preferable to use data from solution studies as no packing effects will disturb the bond distance distribution. It is also better to opt for monodentate homoleptic complexes, monodentate to avoid unwanted straining from the preferred coordination, and homoleptic to remove ligand-related bias, both features being easily attainable in solution. Comparative data are more easily obtained, however, in the large amounts of crystallographic data for solvate structures available in the Cambridge Structural Database (CSD)[8] and the Inorganic Crystal Structure Database (ICSD).[9] These have been reviewed for evaluation of the ionic radii of the lanthanoid(III) ions, in addition to the non-crystallographic structural data available for the hydrated, dmso, and dmpu solvated lanthanoid(III) ions in solution and from solid state data in this study.[6,7,14] Additionally, solvate structures allow for additional geometric configurations with different limiting radius ratios than the traditional ones pertaining to highly ordered inorganic compounds, Table 1. Taken together, this allows for a study over the entire lanthanoid(III) series representing nine-, eight-, seven-, and six-coordination and to a lesser extent also five- and four-coordination.[6,7,10−14,35]

Experimental Section

Solvent. *N,N*′-Dimethylpropyleneurea, (reagent grade, BASF AG) was distilled over calcium hydride, CaH_2, (reagent grade, Merck) at temperatures lower than 400 K under reduced pressure (~6 kPa) and stored in dark glass bottles over 3 Å molecular sieves.

Chemicals. Anhydrous lanthanoid(III) iodides (Aldrich, 99.9+ % or better) were used as purchased. These salts were dissolved to saturation in freshly distilled dmpu carefully heated in an oil bath, not exceeding 323 K, and let to slowly cool to room temperature. The compounds obtained by this procedure were hexakis(dmpu)lanthanum(III) iodide trisolvate (**1**), hexakis(dmpu)cerium(III) iodide trisolvate (**2**), hexakis(dmpu)praseodymium(III) iodide trisolvate (**3**), hexakis(dmpu)neodymium(III) iodide trisolvate (**4**), hexakis(dmpu)samarium(III) iodide (**5**), hexakis(dmpu)gadolinium(III) iodide (**6**), hexakis(dmpu)terbium(III) iodide (**7**), hexakis(dmpu)dysprosium(III) iodide (**8**), hexakis(dmpu)holmium(III) iodide (**9**), hexakis(dmpu)erbium(III) iodide (**10**), hexakis(dmpu)thulium(III) iodide (**11**), hexakis(dmpu)ytterbium(III) iodide (**12**), and hexakis(dmpu)lutetium(III) iodide (**13**). The prepared crystals and solids were kept in their respective mother liquids until the start of the experiments as many of these salts are highly hydroscopic. For europium, anhydrous europium(III) trifluoromethanesulfonate (Aldrich, 98%) was used, as the corresponding europium(III) iodide does not exist because of spontaneous oxidation of iodide to iodine by europium(III).

Crystallography. The crystallographic study only included iodide salts. Data acquisition on **1** was performed at MAX-Lab, Lund University, Sweden, beamline I711 on a Bruker AXS diffractometer with a SMART 1000 CCD detector under cold conditions (100 K). All other crystallographic data collections were performed on an Oxford Diffraction Xcalibur 2 cooling the crystal to 100 K, except for **13** where data were collected at room temperature as well, $\mathbf{13}_{RT}$. Data collection and refinement details are given in Table 2. The structures were solved by the direct methods in SHELX[43] and refined using full-matrix least-squares on F^2. All non-hydrogen atoms were treated anisotropically. The methyl and propylene hydrogen atoms were calculated in ideal positions riding on their respective carbon atom.

EXAFS - Data Collection. The EXAFS measurements were performed at ESRF in Grenoble, France, high energy beamline BM29 (K edge data), Stanford Synchrotron Radiation Lightsource (SSRL), Stanford, U.S.A., beamlines 2−3 and 4−1, (L_{III} edge data), and MAX-Lab, Lund University, Sweden, beamline I811 (L_{III} edge data). Data collection of the K edge data was performed in transmission mode, while the L_{III} edge data were collected simultaneously in transmission and fluorescence mode. The EXAFS station for the K edge measurements was equipped with a Si[511] double crystal monochromator, while for the L_{III} edge measurements Si[111] or Si[220] double crystal monochromators were used. SSRL operated at 3.0 GeV and a maximum current of 100 mA, MAX-lab at 1.5 GeV and a maximum current of 200 mA, and ESRF at 6.0 GeV and a maximum current of 200 mA.

To remove higher order harmonics, the beam intensity was detuned to 35−50% of the maximum intensity at the end of the scans for the L_{III} edge scans (the lower value for the lowest energy) and to 80% for the K edge ones. The energy scales of the X-ray absorption spectra were calibrated by assigning the first inflection point of the K and L_{III} edges of a lanthanoid metal foil, recorded simultaneously, to the values given in the literature.[44] For each sample 3−6 scans were averaged, giving a

---

(33) Lundberg, D.; Ullström, A.; D'Angelo, P.; Persson, I. *Inorg. Chim. Acta* **2007**, *360*, 1809–1818.

(34) Lundberg, D.; Eriksson, L.; D'Angelo, P.; Persson, I. *J. Mol. Liq.* **2007**, *131*, 105–112.

(35) Lundberg, D. *The coordination chemistry of solvated metal ions in DMPU - a study of a space-demanding ligand*; Swedish University of Agricultural Sciences: Uppsala, 2006; p 79.

(36) *DMPU*; BASF: Ludwigshafen, Germany, 1999.

(37) *Safe HMPA Substitutions*; Merck-Schuchardt: Germany, 1984.

(38) Juaristi, E.; Murer, P.; Seebach, D. *Synthesis-Stuttgart* **1993**, 1243–1246.

(39) Mukhopadhyay, T.; Seebach, D. *Helv. Chim. Acta* **1982**, *65*, 385–391.

(40) Ireland, R.; Wipf, P.; Armstrong, J. *J. Org. Chem.* **1991**, *56*, 650–657.

(41) Schmutz, J. F. *Chem. Eng. News* **1978**, *56*, 37–39.

(42) Spencer, H. *Chem. Ind.* **1979**, 728–733.

(43) Sheldrick, G. M. *Acta Crystallogr., Sect. A* **2008**, *64*, 112–122.

(44) Thompson, A.; Attwood, D.; Gullikson, E.; Howells, M.; Kim, K.; Kirz, J.; Lindau, I.; Pianetta, P.; Robinson, A.; Scofield, J.; Underwood, J.; Vaughan, D.; Williams, G.; Winick, H. *X-ray data booklet*, 2nd ed.; Lawrence Berkeley National Laboratory: Berkeley, CA, 2001; p 161.

Table 2. Crystallographic Data of the dmpu Solvated Lanthanoid(III) Complexes **1**, **3**, **4**, **6**, **7**, **10**, **12**, **13**, and $\mathbf{13}_{RT}$

	1	**3**	**4**	**6**	**7**	**10**	**12**	**13**	$\mathbf{13}_{RT}$
formula [a]	$C_{54}H_{108}I_3$-$LaN_{18}O_9$	$C_{54}H_{108}I_3$-$N_{18}O_9Pr$	$C_{54}H_{108}I_3$-$N_{18}NdO_9$	$C_{36}H_{72}GdI_3$-$N_{12}O_6$	$C_{36}H_{72}I_3$-$N_{12}O_6Tb$	$C_{36}H_{72}ErI_3$-$N_{12}O_6$	$C_{36}H_{72}I_3$-$N_{12}O_6Yb$	$C_{36}H_{72}I_3$-$LuN_{12}O_6$	$C_{36}H_{72}I_3$-$LuN_{12}O_6$
M_W	1673.17	1675.17	1678.50	1307.00	1308.67	1317.01	1322.79	1324.71	1324.71
crystal system	hexagonal	hexagonal	hexagonal	monoclinic	monoclinic	monoclinic	monoclinic	monoclinic	monoclinic
space group	$P6_3/m$ (No. 176)	$P6_3/m$ (No. 176)	$P6_3/m$ (No. 176)	$P2_1/n$ (No. 14)	$P2_1/n$ (No. 14)	$P2_1/n$ (No. 14)	$P2_1/n$ (No. 14)	$P2_1/n$ (No. 14)	$P2_1/n$ (No. 14)
a/Å	13.33(1)	13.2345(5)	13.2344(3)	12.2946(1)	12.2250(5)	12.1803(2)	12.1433(1)	12.11482(9)	12.1016(1)
b/Å	13.33(1)	13.2345(5)	13.2344(3)	11.9123(1)	11.9013(6)	11.8634(3)	11.8667(1)	11.86508(8)	12.0872(1)
c/Å	23.32(1)	23.2798(12)	23.2595(3)	17.4121(2)	17.4800(6)	17.5085(4)	17.5867(2)	17.63997(13)	17.9318(2)
α/deg	90	90	90	90	90	90	90	90	90
β/deg	90	90	90	92.039(1)	92.084(3)	91.931(2)	91.898(1)	92.0062(7)	91.8807(11)
γ/deg	120	120	120	90	90	90	90	90	90
V/Å^3	3589(4)	3531.2(3)	3528.09(12)	2548.8(2)	2541.54(19)	2528.54(10)	2532.87(4)	2534.07(3)	2621.55(4)
Z	2	2	2	2	2	2	2	2	2
T/K	100	100	100	100	97	97	100	100	273
ρ_{calc}/Mg m^{-3}	1.548	1.576	1.58	1.703	1.71	1.73	1.735	1.736	1.678
μ	5.982	2.063	2.110	3.169	3.264	3.542	3.725	3.826	3.699
λ/Å	1.087	0.71073	0.71073	0.71073	0.71073	0.71073	0.71073	0.71073	0.71073
θ range/deg	2.70−31.88	3.66−25.67	3.93−30.50	3.73−32.36	3.75−25.03	3.76−25.03	3.77−26.37	3.78−25.02	3.77−25.03
refl. collected	1174	2285	3661	8309	4473	4449	5155	4458	4621
refl. $I > 2\sigma$	1158	1186	3174	5737	1868	2914	4508	4016	3791
compl. θ	0.987	0.993	0.995	0.911	0.996	0.996	0.996	0.997	0.996
GoF	1.083	0.761	1.177	0.868	0.559	0.865	1.055	1.124	1.018
R_1 (all data)	0.0600	0.1146	0.0349	0.0456	0.1147	0.0686	0.0232	0.021	0.0398
final $R_1(I > 2\sigma)$	0.0551	0.0404	0.0287	0.0252	0.0384	0.0393	0.0190	0.0182	0.0275
wR_2 (all data)	0.1375	0.0618	0.0752	0.0513	0.0556	0.0903	0.0472	0.0476	0.0651
min/max	−0.64/1.07	−0.58/0.79	−0.86/1.02	−1.04/0.72	−0.57/0.5	−1.36/2.07	−1.01/0.72	−0.97/1.11	−0.88/0.66

[a] Crystals **1**, **3**, and **4** has the general composition $[Ln(dmpu)_6]I_3 \cdot 3$ dmpu, whereas **6**, **7**, **10**, **12**, **13**, and $\mathbf{13}_{RT}$ has $[Ln(dmpu)_6]I_3$, see Figures 2a and 2b.

satisfactory signal-to-noise ratio. Solid samples were diluted with boron nitride, BN, and pressed into a 1.5 mm silver or brass frame to give an edge step of unity on logarithmic scale. The EXAFS measurements in the solid state included the respective iodide salts (La−Nd, Sm, Gd−Lu) and were carried out at ambient room temperature at the respective synchrotron light facility. The performed crystal diffraction and EXAFS experimental measurements are summarized in Supporting Information, Table S2. Solution samples were measured using brass or titanium cells with thin Mylar film as windows and a Teflon spacer of appropriate thickness to achieve a suitable edge step.

EXAFS - Data Analysis. The EXAFSPAK[45] and GNXAS[46−48] program packages were used for the data treatment. The EXAFS functions were extracted using standard procedures for pre-edge subtraction using the EXAFSPAK program package, then refined with GNXAS. The GNXAS code is based on the calculation of the EXAFS signal and a subsequent refinement of the structural parameters. An anomalous feature, clearly deviating from the oscillations in the scattering pattern and previously assigned to the $2p^4d \rightarrow 5d^2$ double electron transition, is observed at $k \approx 6$ Å^{-1} for the early lanthanoids.[49,50] The GNXAS software does not have a deglitching feature, but erroneous data points can be left out of the calculation with minimal effect on the fitting procedure. The GNXAS method accounts for multiple scattering (MS) paths, with correct treatment of the configurational average of all the MS signals to allow fitting of correlated distances and bond distance variances (Debye−Waller factors). A correct description of the first coordination sphere of the studied complex has to account for asymmetry in the distribution of the ion−solvent distances. Therefore, the Ln−O two-body signals associated with the first coordination shells were modeled with Γ-like distribution functions which depend on four parameters: the CN N, the average distance R, the mean-square variation σ, and the skewness β. The β term is related to the third cumulant C_3 through the relation $C_3 = \sigma^3\beta$, and R is the first moment of the function $4\pi \int g(r) r^2 \, dr$. It is important to stress that R is the average distance and not the position of the maximum of the distribution (R_m).

The standard deviations given for the refined parameters are obtained from k^2 weighted least-squares refinements of the EXAFS function $\chi(k)$, and do not include systematic errors of the measurements. These statistical error estimates provide a measure of the precision of the results and allow reasonable comparisons, for example, of the significance of relative shifts in the distances. However, the variations in the refined parameters, including the shift of the E_o value (for which $k = 0$), using different models and data ranges, indicate that the absolute accuracy of the distances given for the separate complexes is within ±0.005 to 0.02 Å for well-defined interactions. The "standard deviations" given in the text have been increased accordingly to include estimated additional effects of systematic errors.

Results

Crystal Structures of $[Ln(C_6H_{12}N_2O)_6]I_3 \cdot 3C_6H_{12}N_2O$, Ln = La, Pr, Nd. The crystal structures of hexakis(dmpu)lanthanum(III) (**1**), -praseodymium(III) (**3**), and -neodymium(III) (**4**) iodide trisolvate are isostructural and crystallize in the hexagonal space group $P6_3/m$

---

(45) George, G. N.; Pickering, I. J. *EXAFSPAK - A suite of computer programs for analysis of X-ray absorption spectra*; Stanford Synchrotron Radiation Laboratory: Stanford, CA, 2000; p 56.

(46) Filipponi, A.; Di Cicco, A. *Phys. Rev. B* **1995**, *52*, 15135–15149.

(47) Filipponi, A.; Di Cicco, A. *Task Quarterly* **2000**, *4*, 575–669.

(48) Filipponi, A.; Di Cicco, A.; Natoli, C. R. *Phys. Rev. B* **1995**, *52*, 15122–15134.

(49) Solera, J.; Garcia, J.; Proietti, M.; Sanchez, M. *Physica B* **1995**, *208*, 71−72.

(50) Solera, J.; Garcia, J.; Proietti, M. *Phys. Rev. B* **1995**, *51*, 2678–2686.

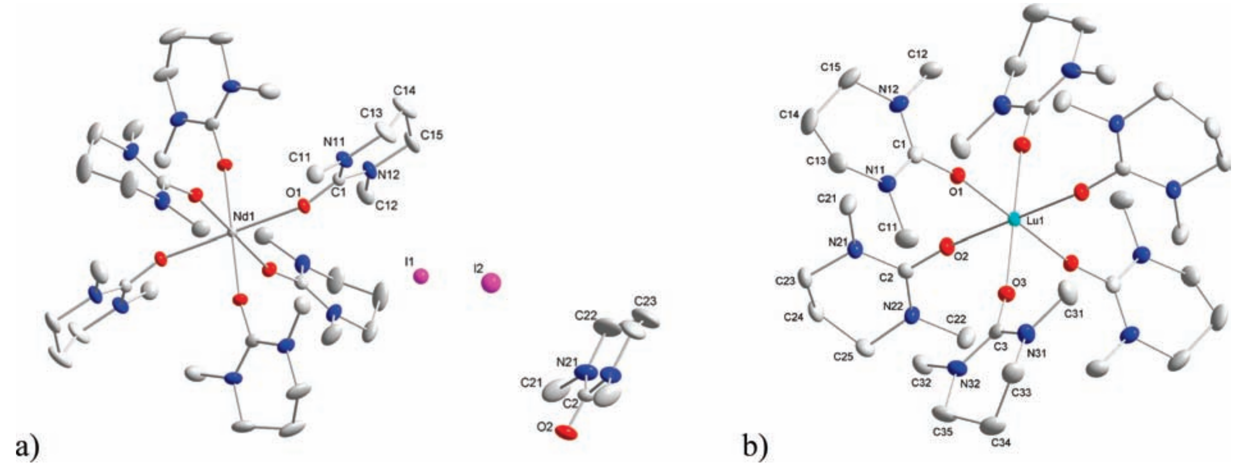

Figure 2. (a) Projection of the cation/solvent component, counterions, and solvate ligand for the hexagonal complex **4**. Thermal ellipsoids are at 50% probability. Hydrogen atoms are omitted for clarity; all symmetric ligand molecules have been added. The Nd−O bond distance is 2.319(2) Å and the Nd−O−C bond angle is 160.7(2)°. (b) Projection of the cation/solvent component for the monoclinic complex **13**. Thermal ellipsoids are at 50% probability. Hydrogen atoms are omitted for clarity; all symmetric ligand molecules have been added. The bond distances (in Å) are Lu−O1 2.1797(15), Lu−O2 2.181(2), and Lu−O3 2.180(2). The average Lu−O−C bond angle is 166.8(2)°.

(No. 176), $Z = 2$; unit cell dimensions and refinement parameters are summarized in Table 2. The unit cell contains two discrete $[Ln(C_6H_{12}N_2O)_6]^{3+}$ complexes, six iodide ions, and six non-coordinated dmpu molecules. The lanthanoid(III) ion, located on a 3-fold axis, coordinates to the oxygen atom of the dmpu molecules in a regular LnO_6 octahedron (Figure 2a), with O−Ln−O angles either 90.0(3) or 180°. The hexagonal symmetry confines the Ln−O bond distances to be equidistant at 2.368(4), 2.342(5), and 2.319(2) Å for **1**, **3**, and **4**, respectively. The Ln−O−C angle, about 160.5°, is significantly larger than the corresponding angle found in dmpu solvates of softer metal ions, but slightly lower than those previously reported for samarium(III)[51] and ytterbium(III).[52] The ring structures of the coordinated dmpu molecules are more or less in the same plane, with the exception of the middle propylene carbon which deviates with a dihedral angle of about 50°. Each ring structure is tilted by 25(2) and 65(2)° based on the dihedral angle between the nitrogens and the straight O−Ln−O angles perpendicular to the ligand (Supporting Information, Figure S1a). The non-coordinated dmpu molecule is symmetrically bisected through the oxygen (O2), carbonyl carbon (C2), and middle propylene carbon (C23).

Crystal Structures of $[Ln(C_6H_{12}N_2O)_6]I_3$, Ln = Gd, Tb, Er, Yb, Lu. The crystal structures of hexakis(dmpu)gadolinium(III) (**6**), -terbium(III) (**7**), -erbium(III) (**10**), -ytterbium(III) (**12**), and -lutetium(III) (**13, 13_{RT}**) iodide are isostructural and crystallize in the monoclinic space group $P2_1/n$ (No. 14), $Z = 2$; unit cell and refinement parameters are summarized in Table 2. The unit cell contains two discrete $[Ln(C_6H_{12}N_2O)_6]^{3+}$ complexes and six individual iodide ions. In the $[Ln(C_6H_{12}N_2O)_6]^{3+}$ complexes, the lanthanoid(III) ion is in the center of a regular LnO_6 octahedron, with angles of either 90.0(15) or 180° and average bond distances falling from 2.264(2) to 2.181(2) Å for **6** to **13**, Figure 2b. The Ln−O−C bond angle for these solvates crystallizing in monoclinic space group is even larger than those in the hexagonal ones, with values from 164.6(2) to 166.8(2)° over the series. Each dmpu ring structure is tilted by 17(2) and 68(2)° based on the dihedral angle between the nitrogens and the straight O−Ln−O angles perpendicular to the respective ligand (Supporting Information, Figure S1b).

The room temperature study of hexakis(dmpu)lutetium(III) iodide (**13_{RT}**) shows a slightly higher mean Ln−O−C bond angle, 169.4(2)°, but lies in the same range as the previously reported values for hexakis(dmpu)samarium(III)[51] and -ytterbium(III)[52] compounds as well as for the lanthanoid-like hexakis(dmpu)scandium(III)[53] and -yttrium(III)[54] iodides. On the basis of the available data, increased temperature leads to a slightly larger bond angle, whereas the Ln−O bond distance is not significantly affected.

EXAFS Studies of Solid Hexakis(dmpu)lanthanoid(III) Iodide Salts, 1−13. A comparison of the experimental and theoretical EXAFS signals of the solid hexakis(dmpu)lanthanoid(III) iodides is given in Figure 3 (L_{III} edge data). The analysis has been carried out starting from the crystallographic structures including all of the atoms within a distance of about 4 Å from the photoabsorbing atom. The Ln···C single scattering, the Ln−O−C three-leg scattering, and other multiple scattering (MS) pathways within the LnO_6 core have all been found to provide a detectable contribution to the EXAFS signal. The presence of a significant contribution from the MS within the LnO_6 core strongly indicates that the dmpu solvated lanthanoid(III) ions have more or less regular octahedral configurations. During the refinement procedures, the Ln−O−C bond angles were refined within the range 160−167° in all samples.

The best-fit Ln−O bond distances obtained from the analysis decrease smoothly with increasing atomic number of the lanthanoid(III) ion and are in close agreement

---

(51) Nishiura, M.; Okano, N.; Imamoto, T. *Bull. Chem. Soc. Jpn.* **1999**, *72*, 1793–1801.

(52) Mikami, K.; Kotera, O.; Motoyama, Y.; Tanaka, M. *Inorg. Chem. Commun.* **1998**, *1*, 10–11.

(53) Lindqvist-Reis, P. *Structure of solvated metal ions: Solution and crystal structure of Ga^{3+}, In^{3+}, Sc^{3+}, Y^{3+}, La^{3+} and Ca^{2+} ions with water and non-aqueous oxygen donor solvents*; KTH: Stockholm, 2000; p 57.

(54) Lindqvist-Reis, P.; Näslund, J.; Persson, I.; Sandström, M. *J. Chem. Soc., Dalton Trans.* **2000**, 2703–2710.

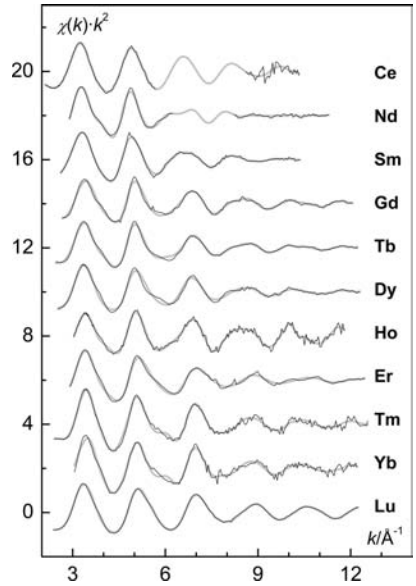

Figure 3. Comparison between the best-fit theoretical EXAFS signal (gray line) and experimental data (thin black line) of L_{III} edge spectra of solid hexakis(dmpu)lanthanoid(III) iodide. The parts of the experimental data for cerium(III) and neodymium(III) that are affected by $2p^4d \rightarrow 5d^2$ double electron excitation (refs 49 and 50) have been removed for clarity and not included in the fitting.

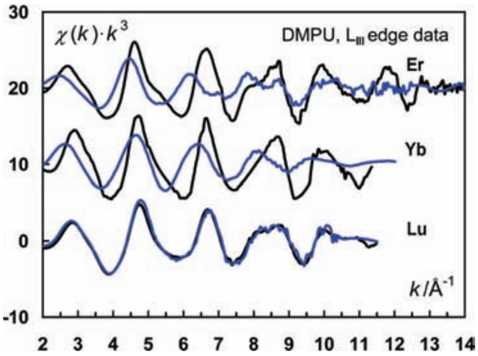

Figure 4. Comparison of experimental L_{III} edge EXAFS functions of solid hexakis(dmpu)erbium(III), -ytterbium(III), and -lutetium(III) iodide (black lines) and the dmpu solutions of erbium(III), ytterbium(III), and lutetium(III) iodide (blue lines). The identical EXAFS wave function for lutetium(III) is taken as evidence that the coordination and configuration are identical in solution and solid state. The *k* weighting has been increased to k^3 to augment the differences seen between the six- and seven-coordinate systems.

with those obtained from crystallography, Supporting Information, Table S3. As the EXAFS studies were performed at ambient room temperature, the flexibility in bond lengths and angles are expected to be larger than those in the crystallographic data collected at 100 K.

Structure of the dmpu Solvated Lanthanoid(III) Ions in Solution. The EXAFS functions of the solid hexakis(dmpu)lutetium(III) iodide and the dmpu solution of lutetium(III) iodide are identical showing that the dmpu solvated lutetium(III) ion is octahedral also in solution. The EXAFS functions for all other dmpu solutions of lanthanoid(III) iodide/trifluoromethanesulfonate are, however, significantly different from the corresponding solid solvate (Figure 4 and Supporting Information, Figure S2ab). Taken together, this is a strong evidence that the dmpu solvated lanthanoid(III) ions have different configuration in solution and in the solid state, as previously seen for lanthanum.[55] The contribution of the Ln−O−C signal is significant and has to be included, though completely free refinement of a subordinate parameter was not possible. With the knowledge obtained from the crystallographic study and the lutetium(III) data in solution and solid state, we have opted for a refined value within the 160−170° range in the data treatment.

The data analysis showed that the mean Ln−O bond distance is more than 0.08 Å longer in solution than in the solid state. Furthermore, the bond distances in solution are almost 0.1 Å shorter than expected for eight-coordinate complexes.[8,9,13,14] Additionally, the Ln···C single and Ln−O−C triple scattering pathways both give significant contributions to the EXAFS functions, but no further MS contribution, for example, from the inner-core, is present, signifying that the symmetry of the dmpu solvated lanthanoid(III) ions in solution is low, CN ≠ 6. This ultimately means that the dmpu solvated lanthanoid(III) ions, except lutetium(III), unquestionably are seven-coordinate in dmpu solution. The Ln−O−C bond angles are close to 160°, as in the solid solvates. It is not possible from the present data to discern whether these seven-coordinate lanthanoid(III) solvates have monocapped trigonal prismatic, monocapped octahedral, or pentagonal bipyramidal configuration. The structure parameters from the refinements of the EXAFS data are summarized in Table 3, and the fits of K and L_{III} edge data are given in Figures 3, 4, and Supporting Information, Figures S2a−c. This study also implies that the dmpu solvated yttrium(III) ion in solution is likely seven-coordinate rather than six-coordinate as previously suggested,[55] once again stressing the need to make comparisons between solution and solid state when using EXAFS as the primary or sole investigation technique.

Discussion

DMPU Solvated Lanthanoid(III) Ions. It is obvious that dmpu is a space-demanding ligand upon coordination since the expected CN eight (CN = 8) is *not* seen in any of the dmpu solvated lanthanoid(III) ions. Accommodating seven ligands has repercussions on the crystalline state, since such complexes cannot benefit from the symmetry-related lattice energy gain found in both eight- and six-coordinate structures. This has the supplementary effect that the lowering of the CN is continued one step further for all crystallized solvates, while the seven-coordination is retained in solution where such driving forces are not present. Similar changes have been seen for zinc(II) dmpu solvates for transitions between the crystallographically more stable four-coordinate complex and its five-coordinate counterpart in solution.[34]

Another effect brought about by the decrease of the lanthanoid(III) ionic radius is the phase transition of the crystalline compounds from hexagonal to monoclinic unit cell symmetry between neodymium and gadolinium, which alters the environment within the unit cell. The most obvious change is the presence of non-coordinated dmpu ligand molecules in the unit cell of the larger ions, but also includes the shift from a fairly stable Ln−O−C

---

(55) Näslund, J.; Lindqvist-Reis, P.; Persson, I.; Sandström, M. *Inorg. Chem.* **2000**, *39*, 4006–4011.

Table 3. EXAFS Structural Parameters of the *N*,*N*′-dimethylpropyleneurea (dmpu) Solvated Lanthanoid(III) Ions in (a) dmpu Solution and (b) Solid State As Determined by GNXAS[a]

		K edge				L_{III} edge			
		Ln−O	C−O	Ln···C	∠Ln−C−O	Ln−O	C−O	Ln···C	∠Ln−C−O
$[Ce(dmpu)_6]I_3(s)$	*d*					2.348(4) [2.344]	1.275(3)	3.573(10)	162(2)
	σ^2/C^3					0.0108(6)/0.06 $\times 10^{-4}$	0.0026(3)	0.018(2)	
	N					6.0	6.0	6.0	
$[Pr(dmpu)_6]I_3(s)$	*d*	2.342(4) [2.332]	1.275(3)	3.597(8)	162(2)				
	σ^2/C^3	0.0055(3)/1.1 $\times 10^{-5}$	0.0024(3)	0.012(1)					
	N	6.0	6.0	6.0					
$[Nd(dmpu)_6]I_3(s)$	*d*					2.328(4) [2.318]	1.275	3.542(9)	160(2)
	σ^2/C^3					0.0084(4)/1.2 $\times 10^{-5}$	0.0025	0.0089(10)	
	N					6.0	6.0	6.0	
$[Sm(dmpu)_6]I_3(s)$	*d*					2.301(4) [2.298]	1.275	3.558(9)	165(2)
	σ^2/C^3					0.0084(4)/0.5 $\times 10^{-5}$	0.0025	0.0177(9)	
	N					6.0	6.0	6.0	
$[Gd(dmpu)_6]I_3(s)$	*d*	2.269(7) [2.259]	1.275	3.525(9)	165(2)	2.272(4) [2.262]	1.275	3.507(9)	165(2)
	σ^2/C^3	0.0068(4)/0.9 $\times 10^{-5}$	0.0025	0.0154(9)		0.0066(4)/0.7 $\times 10^{-5}$	0.0025	0.0161(9)	
	N	6.0	6.0	6.0		6.0	6.0	6.0	
$[Tb(dmpu)_6]I_3(s)$	*d*	2.256(4) [2.256]	1.275(3)	3.481(8)	165(2)	2.254(2) [2.254]	1.275(3)	3.479(8)	165(2)
	σ^2/C^3	0.0070(4)/0	0.0032(3)	0.0160(8)		0.0072(4)/0	0.0027(3)	0.0165(8)	
	N	6.0	6.0	6.0		6.0	6.0	6.0	
$[Dy(dmpu)_6]I_3(s)$	*d*	2.240(4) [2.240]	1.275	3.487(8)	165(2)	2.238(4) [2.238]	1.275	3.485(9)	165(2)
	σ^2/C^3	0.0072(4)/0	0.0025	0.0162(8)		0.0068(4)/0	0.0025	0.0151(9)	
	N	6.0	6.0	6.0		6.0	6.0	6.0	
$[Ho(dmpu)_6]I_3(s)$	*d*					2.224(4) [2.224]	1.275(3)	3.471(9)	165(2)
	σ^2/C^3					0.0062(4)/0	0.0027(3)	0.0137(8)	
	N					6.0	6.0	6.0	
$[Er(dmpu)_6]I_3(s)$	*d*	2.212(4) [2.212]	1.275	3.451(8)	163(2)				
	σ^2/C^3	0.0065(4)/0	0.0025	0.0145(8)					
	N	6.0	6.0	6.0					
$[Tm(dmpu)_6]I_3(s)$	*d*					2.202(4) [2.202]	1.275	3.449(8)	165(2)
	σ^2/C^3					0.0062(4)/0	0.0025	0.0139(9)	
	N					6.0	6.0	6.0	
$[Yb(dmpu)_6]I_3(s)$	*d*					2.198(2) [2.198]	1.275	3.445(8)	165(2)
	σ^2/C^3					0.0060(4)/0	0.0025	0.0116(8)	
	N					6.0	6.0	6.0	
$[Lu(dmpu)_6]I_3(s)$	*d*					2.177(4) [2.177]	1.275(3)	3.424(8)	163(2)
	σ^2/C^3					0.0066(4)/0	0.0027(3)	0.0167(8)	
	N					6.0	6.0	6.0	

		K edge				L_{III} edge			
		Ln−O	C−O	Ln···C	∠Ln−C−O	Ln−O	C−O	Ln···C	∠Ln−C−O
La^{3+}/dmpu	*D*	2.466(4) [2.453]	1.275	3.680(10)	161(1)	2.454(5) [2.454]	1.275	3.676(13)	159.5(1.5)
	σ^2/C^3	0.0098(4)/0.54 $\times 10^{-4}$	0.0025	0.016(1)		0.0106(8)/0.02·10−4	0.0025	0.016(2)	
	N	7.0	7.0	7.0		7.0	7.0	7.0	
Ce^{3+}/dmpu	*D*	2.441(3) [2.432]	1.275	3.662(9)	160(2)	2.438(5) [2.427]	1.275	3.647(12)	160(2)
	σ^2/C^3	0.0094(3)/0.21 $\times 10^{-4}$	0.0025	0.015(1)		0.0111(5)/0.23·10−4	0.0025	0.016(2)	
	N	7.0	7.0	7.0		7.0	7.0	7.0	
Pr^{3+}/dmpu	*D*	2.420(4) [2.414]	1.275	3.633(10)	160(2)	2.420(4) [2.408]	1.275	3.635(10)	160(2)
	σ^2/C^3	0.0078(4)/0.11 $\times 10^{-4}$	0.0025	0.0105(10)		0.0088(4)/0.14·10−4	0.0025	0.012(1)	
	N	7.0	7.0	7.0		7.0	7.0	7.0	
Nd^{3+}/dmpu	*D*	2.405(4) [2.395]	1.275	3.624(9)	160(2)	2.408(4) [2.397]	1.275	3.623(10)	160(2)
	σ^2/C^3	0.0095(4)	0.0025	0.0150(9)		0.0099(4)/0.19·10−5	0.0025	0.0285(9)	
	N	7.0	7.0	7.0		7.0	7.0	7.0	
Sm^{3+}/dmpu	*D*	2.386(4) [2.377]	1.275	3.586(9)	156(2)	2.380(2) [2.374]	1.275	3.604(8)	160(2)
	σ^2/C^3	0.0086(4)/0.13 $\times 10^{-4}$	0.0025	0.0128(8)		0.0090(4)/0.10·10−4	0.0025	0.0185(9)	
	N	7.0	7.0	7.0		7.0	7.0	7.0	
Eu^{3+}/dmpu	*D*	2.366(4) [2.361]	1.275	3.590(9)	160(2)				
	σ^2/C^3	0.0089(4)/0.08 $\times 10^{-4}$	0.0025	0.0149(9)					
	N	7.0	7.0	7.0					
Gd^{3+}/dmpu	*D*	2.343(4) [2.341]	1.275	3.563(9)	160(2)	2.345(2) [2.343]	1.275	3.568(8)	160(2)
	σ^2/C^3	0.0081(4)/0.02 $\times 10^{-4}$	0.0025	0.021(1)		0.0080(4)/0.02·10−4	0.0025	0.0180(8)	
	N	7.0	7.0	7.0		7.0	7.0	7.0	
Tb^{3+}/dmpu	*d*	2.334(4) [2.334]	1.275	3.571(9)	162(2)	2.332(2) [2.337]	1.275	3.555(9)	160(2)
	σ^2/C^3	0.0082(4)/0	0.0025	0.0167(8)		0.0084(4)/0	0.0025	0.0190(8)	
	N	7.0	7.0	7.0		7.0	7.0	7.0	
Dy^{3+}/dmpu	*d*	2.322(4) [2.322]	1.275	3.537(8)	158(2)	2.324(2) [2.322]	1.275	3.519(8)	159(2)
	σ^2/C^3	0.0082(4)/0	0.0027(3)	0.0167(8)		0.0080(4)/0	0.0025	0.0145(8)	
	N	7.0	7.0	7.0		7.0	7.0	7.0	

Table 3. Continued

		K edge				L_{III} edge			
		Ln−O	C−O	Ln···C	∠Ln−C−O	Ln−O	C−O	Ln···C	∠Ln−C−O
Ho^{3+}/dmpu	*d*					2.311(2) [2.311]	1.275	3.523(8)	158(2)
	σ^2/C^3					0.0087/0	0.0016(3)	0.0169(8)	
	N					7.0	7.0	7.0	
Er^{3+}/dmpu	*d*					2.300(2) [2.300]	1.275	3.517(7)	160(2)
	σ^2/C^3					0.0080(4)/0	0.0025	0.0154(8)	
	N					7.0	7.0	7.0	
Tm^{3+}/dmpu	*d*	2.286(4) [2.286]	1.275	3.507(8)	159(2)	2.284(2) [2.284]	1.275	3.500(8)	160(2)
	σ^2/C^3	0.0085(4)/0	0.0025	0.0152(8)		0.0095(4)/0	0.0025	0.0179(8)	
	N	7.0	7.0	7.0		7.0	7.0	7.0	
Yb^{3+}/dmpu	*d*					2.278(2) [2.278]	1.275	3.503(8)	160(2)
	σ^2/C^3					0.0078(4)/0	0.0025	0.0182(8)	
	N					7.0	7.0	7.0	
Lu^{3+}/dmpu	*d*	2.178(2) [2.178]	1.275	3.425(8)	165(2)	2.178(2) [2.178]	1.275	3.416(7)	165(2)
	σ^2/C^3	0.0065(4)/0	0.0025	0.0121(7)		0.0071(4)/0	0.0025	0.0143(7)	
	N	6.0	6.0	6.0		6.0	6.0	6.0	

[a] In the first column the centroid Ln−O distances (in Å) are reported for an assumed asymmetric distribution represented by the third cumulant parameter C^3 (in $Å^2$); the peak maximum of the Ln−O distribution, R_m, is given within square brackets. Underlined values were fixed during refinement. For the subordinate interaction C−O fixed values of $d = 1.275$ Å and $\sigma = 0.0025$ $Å^2$ were applied if free refinement of the interaction variables was not possible.

bond angle to an increasingly larger one, indicating increased crowdedness along the latter part of the series.

This crystallographic study and those previously performed on hydrates[7,10] and dmso solvates,[13,14] show that the lanthanoid(III) solvate structures normally only crystallize in the highly symmetric configurations, primarily tricapped trigonal prisms (CN = 9), square antiprisms (CN = 8), and, last, octahedrons (CN = 6), as the result of intrinsic lattice effects. Other CNs of solvate complexes do exist, but either in solution where there are no lattice effects or as crystalline compounds with anionic *O*-donor ligands.[8,9] Minor differences between the crystallographic and EXAFS sets can be seen in Figure 3 and Table 3. Some dissimilarity is expected as the experiments were conducted at different temperatures, but has little or no effect on the results on the lanthanoid(III) series as a whole. No significant differences in respect to the bond distances were detected between the EXAFS K and L_{III} data sets.

Ionic Radii of the Lanthanoid(III) Ions. Regardless of CN, the ionic radii of the lanthanoid(III) ions have been shown to decrease smoothly with increasing atomic number, an effect known as the lanthanoid contraction,[56−59] both in monodentate (hydrates) and bidentate complexes because of the identical outer electron shell configuration, $5s^25p^6$, and to relativistic effects.[60,61] The tetrad effect observed in complex formation studies[62] is not seen in the structural investigations, with an example given in Supporting Information, Figure S1 in a lanthanoid(III) study by Persson et al.[7] Quadrelli suggested that this contraction ought to be explained using a quadratic fit,[56] employing Ln−O bond distances derived from three selected crystal series, two complete nine-coordinate hydrate series,[63,64] and one combined mono- and bidentate eight-coordinate study.[65] However, the values of the eight-coordination analysis are based on a study including only four or possibly five elements[65] and not the entire series. This is then, in turn, extrapolated to include seven- and six-coordination, though nothing in the data summarized by Shannon supports the need for a quadratic term, with a linear fit being virtually indistinguishable from a second-order function. Instead, as Shannon points out, the values are derived from non-linear estimations which may help to explain any perceived curvature of the ionic radii.[1] If at all, it may be more appropriate to exclude the lanthanum(III) ion from these comparisons thus improving the already linear trends,[60,61,66] as this ion is lacking 5f electrons. The work by Shannon, and the original one by Shannon and Prewitt, based the ionic radii strictly on inorganic structures with highly symmetric lattices.[1,67] In these oxides, fluorides, and chalcogens, the determining factor in crystal packing is the anionic contribution, where the metal ion assumes its place in the resulting cavities (Supporting Information, Figure S3). In the solvate structures on the other hand, it is the metal ion that influences the rest of the complex, allowing it to obtain its preferred configuration and bond distance more easily. Compared to the cubic and hexagonal close packing (*ccp* and *hcp*, respectively) of the oxide ions, one gets slightly different Ln−O bond distances when compared with solvates of the same CN.[8,9] It is thus reasonable to assume that in this study the bond distances are free from interfering anionic packing contributions which

---

(56) Quadrelli, E. A. *Inorg. Chem.* **2002**, *41*, 167–169.

(57) Seitz, M.; Oliver, A. G.; Raymond, K. N. *J. Am. Chem. Soc.* **2007**, *129*, 11153–11160.

(58) Wells, A. *Structural Inorganic Chemistry*, 5th ed.; Clarendon Press: Oxford, 1984.

(59) Wedepohl, K. H. *Naturwissenschaften* **1996**, *83*, 165–171.

(60) Pyykkö, P. *Chem. Rev.* **1988**, *88*, 563–594.

(61) Clavaguéra, C.; Dognon, J.; Pyykkö, P. *Chem. Phys. Lett.* **2006**, *429*, 8–12.

(62) Powell, K. J. *SC-Database*, v. 5; IUPAC/Academic Software: Sourby Old Farm, Timble, Otley, Yorks, U.K.

(63) Chatterjee, A.; Maslen, E.; Watson, K. *Acta Crystallogr., Sect. B* **1988**, *44*, 381–386.

(64) Gerkin, R.; Reppart, W. *Acta Crystallogr., Sect. C* **1984**, *40*, 781–786.

(65) Abram, U.; Dell'Amico, D. B.; Calderazzo, F.; Della Porta, C.; Merigo, A.; Englert, U.; Marchetti, F. *Chem. Commun.* **1999**, 2053–2054.

(66) Seth, M.; Dolg, M.; Fulde, P.; Schwerdtfeger, P. *J. Am. Chem. Soc.* **1995**, *117*, 6597–6598.

(67) Shannon, R. D.; Prewitt, C. T. *Acta Crystallogr., Sect. B* **1969**, *25*, 925–946.

subsequently affect the estimated ionic radii, making them more appropriate when discussing conventional ionic radii. Furthermore, the proposed ionic radii for the lanthanoid(III) ions in six-, eight-, and nine-coordination reported by Shannon and Prewitt were based almost exclusively on the approximately linear relationship of r^3 versus V_{cell} values in oxides and fluorides. Note that these values were slightly corrected and supplemented with nine values for seven-coordination during Shannon's revision.[1] No ionic radii were given for the lanthanoid(III) ions in four- or five-coordination. Unfortunately, the reported calculated values are intermixed with structurally determined ones, a treatment very common in six- and seven-coordination, making the radii for eight- and nine-coordination the more accurate ones. Care must thus be taken before using Shannon's values as listed; for instance, for the elusive, highly radioactive promethium(III) ion only estimated ionic radii are cited (those originally reported by Greis and Petzel),[68] but they are designated as being equally reliable as many other authentic lanthanoid(III) data. Nevertheless, the citation classics by Shannon and Prewitt, and Shannon, respectively,[1,67,69] were and still are an excellent starting point for comparative coordination chemistry. To allow for comparisons with Shannon's radii, ionic radii for the lanthanoid(III) ions have been calculated by subtracting the radius of a coordinated oxygen atom, 1.34 Å,[70] from the obtained mean Ln−O bond distances, respectively.

Shannon's list of ionic radii shows that there is a strong correlation between CN/geometric configuration and ionic radius.[1] As crystallographic measurements are notably dependable, with bond distances determined within ±0.005 Å or better for well-determined systems, such comparisons are continued here, following the idea that very similar mean M−O bond distances should be found within each CN and configuration within similar types of ligands. The expected (geometrical) CN for lanthanoid(III) ions is eight, which also is reflected in the large amount of such crystallographic data available.[8,9] There is a much smaller number of reported homoleptic complexes for the lower CNs (CN = 4−7), so few in fact that it is hard to draw any conclusions whatsoever *between* different CNs without modifying the ideal homoleptic selection criteria. By allowing neutral heteroleptic monodentate *O*-donors ligands as well, one significantly increases the number of available complexes for all CNs, including CN = 8. It turns out that the eight-coordinate heteroleptic lanthanoid(III) compounds indeed are indistinguishable from their homoleptic counterparts, almost regardless of oxygen donor (Supporting Information, Figure S4a). This was taken as evidence for the robustness of the adjusted expanded method and used for extrapolation to increase the number of complexes for the other CNs included in the study.

Once these large amounts of data have been compiled, they serve as the foundation from which conclusions can be drawn, as well as allowing one to regard large deviations from expected bond lengths as erroneous. The data set for CN = 8, being by far the largest of the ones studied, was used in the statistical calculation for an acceptable range of the Ln−O distance variation. A recursive two-tailed Grubb's test ($P = \pm\ 0.025$), which led to the exclusion of 13 out of 129 values, was applied before calculating the linear slope expected for the lanthanoid contraction. It should be pointed out that with the exception of four abnormally deviating values (CSD codes LADLIM, MEWSIQ, AZEBIQ, and MIDFOU),[8] the congruent linear trend of the lanthanoid contraction is virtually unaffected even *if* statistically rejected values at the chosen probability are included (Supporting Information, Table S4). The remaining values are within ±0.03 Å from the combined trendline of the entire series, and this range was transferred as limits for the other CNs. The congruent trend shows that the anticipated radius of the donating oxygen atom is very similar in almost all neutral monodentate *O*-donating ligands including water. One notable exception is found in solvates which include the cyclic ether tetrahydrofuran (thf). The average bond distances are 0.03 to 0.05 Å longer than observed for other *O*-donor ligands in four- and six-coordination, respectively (Supporting Information, Figure S4b). For five-, seven-, and eight-coordinate structures, the corresponding bond distances are also longer, but the limited number of complexes makes it hard to make reliable comparisons. This is caused by the significantly longer Ln−O bond distance of the thf ligands. The explanation for the markedly different coordination properties seen in thf can be ascribed to the strained ring structure causing the oxygen bonding orbitals to behave in a way not seen in any other ligand, ether or not.[40,71] It is also worth noticing that thf offers a chemically reducing environment, and is therefore used to keep polyvalent transition metals in their reduced form, for example, samarium(II) and ytterbium(II).[8] For these reasons, in addition to the statistical exclusion, *all* crystal structures containing thf and other ethers have been excluded in this study.

When comparing different neutral oxygen donor ligands, molecules with built-in steric hindrance around the coordinating oxygen atom such as tetrasubstituted ureas are regarded as space-demanding upon coordination, while smaller molecules such as water, dmso, and dmf with less or no such obstruction are not. Regardless of their spatial requirements, oxygen atoms that are part of neutral ligand molecules are assumed to maintain the same radius, 1.34 Å,[70] because of their similar electronic environment when forming metal complexes as *O*-donors. This radius is more appropriate than that suggested by Pauling, 1.40 Å,[4] which is based on limiting radius ratios in highly structured oxides. Pauling's value is still more appropriate to use when dealing with oxides with the oxygen as a divalent ion, and this also explains why this value is the one listed for six-coordinate O^{2-} in Shannon and Prewitt's study[67] as well as in Shannon's revised and extended one,[1] as both these articles were based on such structures. In addition, the M−O bond distance in hydroxide structures should be somewhere in between these values and this turns out to be true as Shannon lists it at

---

(68) Greis, O.; Petzel, T. *Z. Anorg. Allg. Chem.* **1974**, *403*, 1–22.

(69) Garfield, E. *Curr. Contents* **1981**, *5*, 281.

(70) Beattie, J. K.; Best, S. P.; Skelton, B. W.; White, A. H. *J. Chem. Soc., Dalton Trans.* **1981**, 2105–2111.

(71) Penczek, S.; Kubisa, P.; Matyjaszewski, K. In *Cationic Ring-Opening Polymerization of Heterocyclic Monomers*; Springer-Verlag: Berlin, 1980; Vol. *37*, pp 3−7.

1.37 Å.[1] A similar effect can be seen in the lanthanoid(III) complexes coordinating monodentate *O*-donor counter-ions and are, for matters of completeness, shown and listed separately for each CN. The linear trend results in ionic radii that are close to those reported by Shannon with an increasing divergence for the end points of the series; see the individual CNs below.

CN 9, Tricapped Trigonal Prism, *ttp*. Nine-coordination is limited to small ligand molecules, and for Sm−Lu it is only observed in hydrates (Supporting Information, Table S5a), most probably because of the extensive hydrogen bonding offered by the *ttp* configuration.[7,10] The structures of the hydrated lanthanoid(III) ions are identical, basic *ttp* configuration, in aqueous solution and the solid trifluoromethanesulfonate salts as shown by EXAFS and XANES studies.[6,7,10,11] However, the behavior of the capping water molecules differs considerably. In the hydrates of the lighter lanthanoids, La−Nd, the capping water molecules are equally strongly bound, while for Sm−Ho, it has been shown that one of the capping water molecules is more strongly bound than the remaining two.[6,7,10,11] This difference in bond strength increases with increasing atomic number, and starting from holmium the difference in bond strength becomes so significant that full occupation of the weakly bound capping water molecule positions is not obtained, ending with lutetium on average binding only 2.2 capping water molecules.[10,11] As a consequence, the bond distances found will differ from values without loss of water, but the configuration remains *ttp*. This in turn affects the predicted ionic radii for regular nine-coordination from holmium to lutetium, and can consequently not be determined directly and must be extrapolated (Figure 5).

CN 8, Square Antiprism, *sap*. The dmso solvated lanthanoid(III) ions have all been found to be eight-coordinate in a square antiprismatic (*sap*) fashion in the solid iodide salts and in dmso solution.[13,14] Similarly, the trimethyleneurea (tmu) solvated lanthanoid(III) trifluoromethanesulfonate salts are also all eight-coordinate.[51] Additionally, many separate eight-coordinate lanthanoid(III) complexes with dmf have been reported by several groups, including lanthanum, cerium, neodymium, europium, gadolinium, terbium, erbium, and holmium.[19,72−78] In addition, there are a large number of independent studies on other eight-coordinate homoleptic lanthanoid(III) solvate complexes with monodentate *O*-donors in the two crystal structure databases,[8,9] all listed by their respective reference code in Supporting Information, Table S5b, forming, more or less, a complete picture of this configuration (Figure 6).

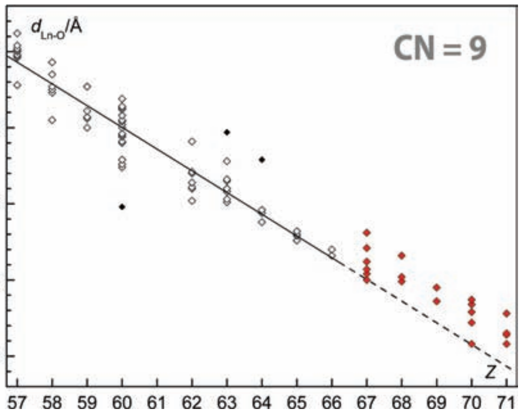

Figure 5. Mean Ln−O bond distances for the nine-coordinate homo- and heteroleptic structures (empty diamonds) reported (refs 8 and 9). Four structures (4%) deviate more than the resulting ±0.03 Å from the least-squares regression line. Loss of capping water ligands affect the mean Ln−O bond distances for Ho−Lu (red diamonds), resulting in a tricapped trigonal prismatic configuration with CN < 9. The reported values should thus not be treated as true nine-coordinate ones.

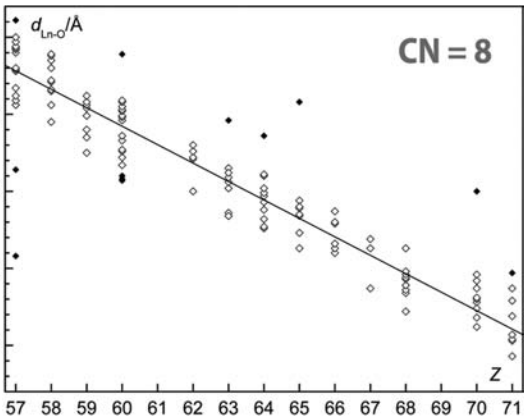

Figure 6. Mean Ln−O bond distances for the eight-coordinate homo- and heteroleptic structures (empty diamonds) reported (refs 8 and 9). Thirteen structures (10%) deviate more than the resulting ±0.03 Å from the least-squares regression line (solid line; recursive Grubb's test, $P = \pm 0.025$) and were excluded (black squares).

Four values, as previously mentioned, are clear outliers which warrants for removal when calculating the first proper average value. Through statistical analysis, nine additional values deviate more than expected from a linear relationship ($P = \pm 0.025$), and were not included in the calculation of the allowed variation in the lanthanoid contraction. The distribution (±0.03 Å) resulting from the combined least-squares regression linear fit was chosen as the limits for the other CNs where a statistical analysis was not possible, and showed that a linear fit is sufficient to describe the reported data.

CN 7, Monocapped Trigonal Prism/Octahedron *mtp*/*mO$_h$*; Pentagonal Bipyramid, *pbp*. There are very few seven-coordinate crystalline lanthanoid(III) solvate structures reported in the literature.[8,9] This is explained by the fact that seven-coordination cannot offer any highly symmetric arrangement in the unit cell which is advantageous from a lattice energy perspective. Furthermore, out of the 20 structures reported, 3 lie outside the ±0.03 Å distribution range and 15 of the accepted ones are samarium(III), erbium(III), and ytterbium(III) structures, involuntarily biasing the data (Supporting Information, Table S5c). However, even for this highly selective material, it is

---

(72) Berthet, J.; Thuéry, P.; Ephritikhine, M. *Polyhedron* **2006**, *25*, 1700–1706.

(73) Chen, L.; Wu, X.; Gao, X.; Zhang, W.; Lin, P. *J. Chem. Soc., Dalton Trans.* **1999**, 4303–4307.

(74) Harrowfield, J. M.; Skelton, B. W.; White, A. H.; Wilner, F. R. *Inorg. Chim. Acta* **2004**, *357*, 2358–2364.

(75) Huang, Q.; Wu, X.; Lu, J. *Polyhedron* **1997**, *16*, 833–838.

(76) Jobic, S.; Poirier-Coutansais, S.; Evain, M.; Brec, R. *Mater. Res. Bull.* **2001**, *36*, 2637–2647.

(77) Liu, S.; Meyers, E. A.; Shore, S. G. *Angew. Chem., Int. Ed.* **2002**, *41*, 3609–3611.

(78) Liu, S.; Plecnik, C. E.; Meyers, E. A.; Shore, S. G. *Inorg. Chem.* **2005**, *44*, 282–292.

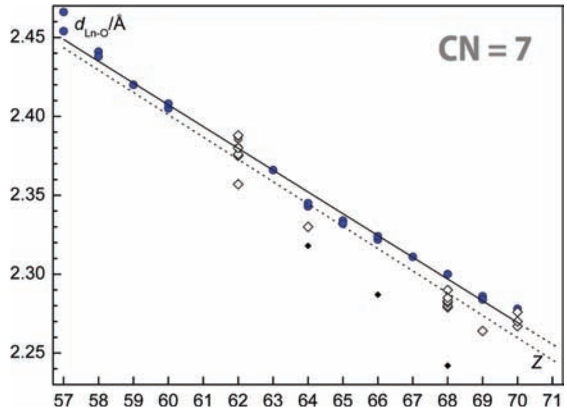

Figure 7. Mean Ln−O bond distances for the reported seven-coordinate crystallographic homo- and heteroleptic structures (empty diamonds) (refs 8 and 9), and K and L_{III} edge solution EXAFS data (blue circles). Three crystal structures (15.0%) deviate more than ±0.03 Å from the least-squares regression line (dashed line) and were excluded (black diamonds). The solution data, free from lattice effects, show Ln−O bond distances up to 0.01 Å longer than the crystallographic set (solid line) which were used for calculating the new ionic radii.

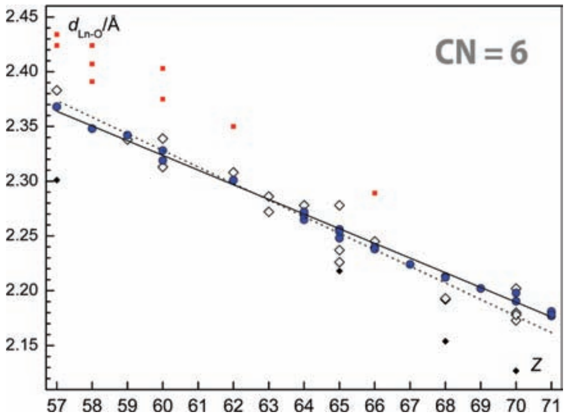

Figure 8. Mean Ln−O bond distances for the six-coordinate homo- and heteroleptic structures (empty diamonds) and K and L_{III} edge EXAFS data (blue circles). Four structures (18.2%) deviate more than ±0.03 Å from the least-squares regression line (solid) and were excluded (black diamonds). The previously reported crystallographic data (refs 8 and 9) agree fairly well with the EXAFS data from dmpu solvated lantanoid(III) ions. The excluded thf coordinating structures (red squares), however, clearly deviate from other solvate structures and were not included in the calculation for new and improved ionic radii.

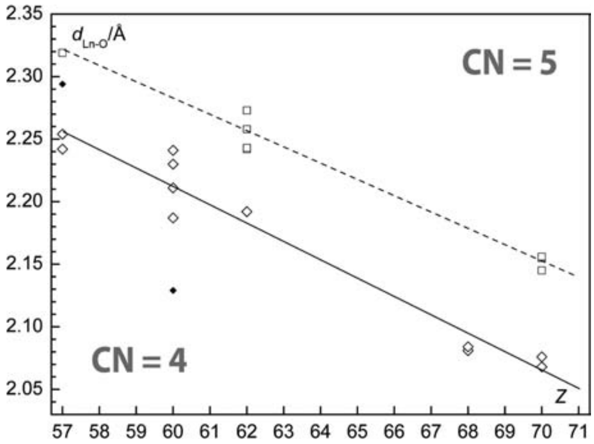

Figure 9. Mean Ln−O bond distances for all four- and five-coordinate homo- and heteroleptic anionic ligands (empty diamonds and squares, respectively) reported (refs 8 and 9). Two structures (14.3%) deviate more than ±0.03 Å from the least-squares regression line (solid line) in the four-coordinate set and were excluded (filled diamonds). All unique five-coordinate structures were kept for its regression line (dashed line).

possible to extrapolate the trend for the entire lanthanoid(III) series, albeit likely with slightly higher margin of error.

The picture of the ionic radii for seven-coordinate complexes is therefore compiled from solution data in this study, as they are free from lattice effects. Results from K and L_{III} edge solution data are effectively indistinguishable, and both sets show Ln−O bond distances that are, on average, up to 0.01 Å longer than those determined from the crystal structures (Figure 7, Supporting Information, Tables S3, and Table 3).

CN 6, Octahedron, O_h. Though having the possibility of forming highly symmetric crystals, six-coordinate lanthanoid(III) solvate structures are almost equally uncommon as their seven-coordinate counterparts, but are at least spread over the entire series (Figure 8, Supporting Information, Table S5d). Four of the 22 crystal structures lie outside the ±0.03 Å range, but 10 of the lanthanoid(III) ions are nevertheless represented. The Ln−O bond distances of the dmpu solvated solid structures and the EXAFS data for lutetium(III) in solution in this study add a significant amount to this number. The previously individually reported structures follow a similar lanthanoid contraction trend as the present crystallographic and EXAFS data, though least-squares fits reveal a slight deviation in the end of the series. However, when calculating the new predicted ionic radii, both sets were included as there is no statistical reason to exclude any additional data point.

CN 5, Trigonal Bipyramid, *tbp*; Square Pyramid, *sqpy*; and CN 4, Tetrahedron, T_d. The very limited amount of data for these two CNs makes it hard to draw firm conclusions regarding ionic radii. Also, there are no reported structures for lanthanoid(III) ions with neutral oxygen donors, but only a small number of complexes with *O*-donating anions for a limited number of lanthanoid(III) ions, 14 structures for CN = 4 and 9 unique ones for CN = 5. Nevertheless, the well-known lanthanoid contraction is, as expected, also seen in these low CNs (Figure 9, Supporting Information, Table S5e).

Proposed New Ionic Radii of the Lanthanoid(III) Ions. To be able to compare the results from this dmpu and database study with those reported by Shannon,[1] the ionic radii for each of the lanthanoid(III) ions have been calculated by subtracting the radius of the coordinated oxygen atom, 1.34 Å,[70] from the respective calculated average Ln−O bond distance. For six-coordination, the results are close to those of Shannon with a trend of increased divergence in the end of the series. This is likely due to the type of strictly O^{2-} matrix-based structures Shannon and Prewitt, as well as Shannon alone, based their radii on.[1,67] For seven-coordination, the results show that Shannon's values underestimate the ionic radii of more or less all lanthanoid(III) ions. The ionic radii presented in this work originate from solution measurements, and are thus free from lattice energy effects. For eight-coordination, the lighter lanthanoid(III) ions (La−Sm) have smaller radii than those listed by Shannon,

Table 4. Summary of Ionic Radii of Lanthanoid(III) Ions Listed by Shannon for Six-, Seven-, Eight-, and Nine-Coordination, $r_{\mathrm{ion,Sh}}$ (ref 1), and the Corresponding Least-Squares Linear Fit Ionic Radii, r_{ion}[a]

	CN = 6		CN = 7		CN = 8		CN = 9	
	$r_{\mathrm{ion,Sh}}$/Å	r_{ion}/Å	$r_{\mathrm{ion,Sh}}$/Å	r_{ion}/Å	$r_{\mathrm{ion,Sh}}$/Å	r_{ion}/Å	$r_{\mathrm{ion,Sh}}$/Å	r_{ion}/Å
La^{III}	1.032	1.027	1.10	1.109	1.160	1.138	1.216	1.203
Ce^{III}	1.01	1.013	1.07	1.095	1.143	1.126	1.196	1.189
Pr^{III}	0.99	0.999		1.081	1.126	1.114	1.179	1.175
Nd^{III}	0.983	0.985		1.067	1.109	1.102	1.163	1.160
Pm^{III}	0.97	0.971[b]		1.054[b]	1.093	1.090[b]	1.144	1.146[b]
Sm^{III}	0.958	0.957	1.02	1.040	1.089	1.078	1.132	1.132
Eu^{III}	0.947	0.943[b]	1.01	1.026	1.066	1.066	1.120	1.117
Gd^{III}	0.938	0.929	1.00	1.012	1.053	1.054	1.107	1.103
Tb^{III}	0.923	0.915	0.98	0.998	1.040	1.042	1.095	1.089
Dy^{III}	0.912	0.901	0.97	0.984	1.027	1.030	1.083	1.075
Ho^{III}	0.901	0.887		0.971	1.015	1.018	1.072	*c*
Er^{III}	0.893	0.873	0.945	0.957	1.004	1.007	1.062	*c*
Tm^{III}	0.88	0.859		0.943	0.994	0.995	1.052	*c*
Yb^{III}	0.868	0.845	0.925	0.929	0.985	0.983	1.042	*c*
Lu^{III}	0.861	0.831		0.916[b]	0.977	0.971	1.032	*c*

[a] In this work and refs 6−13 (Supporting Information, Tables S5a-e) assuming an atomic radius of 1.34 Å for coordinated oxygen (ref 70) for all included *O*-donor ligands. The values for seven-coordination are taken solely from this work, in an effort to avoid lattice effects. [b] No experimental value obtained; all values for Pm^{III} and the Eu^{III} value for CN = 6 are determined by interpolation, and the Lu^{III} value for CN = 7 is determined by extrapolation. [c] Partial loss of capping waters, reduce the CN to 8.91 for Ho^{III}, 8.95 for Er^{III}, 8.8 for Tm^{III}, 8.7 for Yb^{III}, and 8.2 for Lu^{III}. The resulting ionic radii for these intermediate CNs are 1.073, 1.066, 1.051, 1.036, and 1.024 Å, respectively. The corresponding theoretically extrapolated values for CN = 9 are 1.060, 1.046, 1.032, 1.018, and 1.003 Å, respectively.

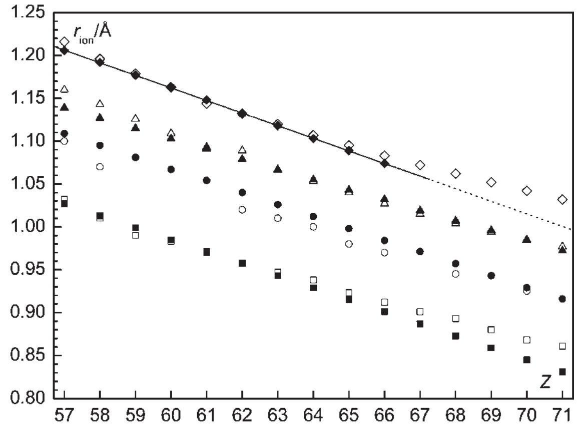

Figure 10. Overview of the ionic radii for lanthanoid(III) ions calculated in this combined dmpu/database study (black symbols) compared to the radii given by Shannon (ref 1; empty symbols) in six- (squares), seven- (circles), eight- (triangles), and nine-coordination (diamonds, solid line). Partial loss of capping waters, prevent determination of ionic radii for nine-coordinate (dashed line) holmium(III), erbium(III), thulium(III), ytterbium(III), and lutetium(III).

but otherwise follows those values closely. For nine-configuration, Shannon's values deviate significantly from the extrapolated nine-coordinate values.[6] The predicted radii are shown together with the ones established for seven-coordination in this study and those listed by Shannon, Table 4 and Figure 10.

When the ionic radii for the lanthanoid(III) series are plotted against atomic number, the familiar lanthanoid contraction can be seen for all CNs including the CN values of 4 and 5 (Figures 5-9). The partial loss of water in the hydrate structures of the heavier lanthanoid(III) ions prevent safe prediction of the ionic radii of holmium(III) to lutetium(III). The same could be argued for the seven-coordinate lutetium(III) ion, but extrapolation is nevertheless included for matters of completeness. The limited number of available structures in four- and five-coordination makes it harder to evaluate the ionic radii for these CNs, but the linear fits in Figure 9 can act as guidelines for an expected value.

The incremental change of the ionic radii in the lanthanoid(III) ions allows for safe prediction of the coordination properties of the highly elusive radioactive promethium(III) ion, without having any experimental data available for comparison (Figure 10). The promethium(III) ion will certainly, just like the neighboring lanthanoid(III) ions, coordinate six and seven dmpu molecules in solid state and solution, respectively. The corresponding CN for promethium(III) with dmso will be eight in both solution and solid states, and correspondingly a full nine-coordination in a *ttp* arrangement for the hydrated promethium(III) ion in aqueous solution. The corresponding ionic radii for promethium(III) can be found in Table 4.

Conclusions

The dmpu solvated lanthanoid(III) ions are seven-coordinate in solution, except lutetium(III), which is six-coordinate. However, the solid solvates precipitating from saturated solutions are all six-coordinate with a significantly shorter Ln−O bond distance compared to what is observed in solution, again with the exception of lutetium(III). The reason for this behavior is certainly due to the larger lattice energies in the octahedral lanthanoid(III) complexes, with relatively high symmetry, in comparison with the seven-coordinate complexes. This also shows that small amounts of the six-coordinate complexes must be present in solution, even though the seven-coordinate complexes are strongly dominating.

A comparison of Ln−O bond lengths in a large number of lanthanoid(III) complexes with neutral oxygen donor ligands and different configurations and CNs has shown that the radius of the oxygen atom is the same as in coordinated water, 1.34 Å,[70] except for (cyclic) ethers.[40,71]

The well-known lanthanoid contraction is seen in the plots for all studied CNs (CN = 4−9) as a steadily decreasing Ln−O bond distance over the series (Figures 5-9). As expected, the bond distances are specific for each CN, observed as increasing bond distances with increasing CNs. Improved ionic radii are given for the first half of the six-coordinate lanthanoid(III) ions, and new radii are suggested for the latter half which are significantly different from those listed by Shannon (Figure 10 and Table 4).[1] Similarly, for seven-coordination, new and improved radii are proposed for all lanthanoid(III) ions, including an extrapolated one for lutetium(III). Corresponding values for eight- and nine-coordinate lanthanoid(III) ions are listed in the aforementioned articles.

Acknowledgment. We gratefully acknowledge the Swedish Research Council, and the SLU fund for internationalization of postgraduate studies for financial support (D.L.), and BASF AG for supplying the solvent *N,N′*-dimethylpropyleneurea. Portions of this research were carried out at the Stanford Synchrotron Radiation Lightsource (SSRL), the European Synchrotron Radiation Facility (ESRF), Grenoble, France, and the MAX-Lab synchrotron radiation source at Lund University, Sweden, which all are acknowledged for the allocation of beam time and laboratory facilities. SSRL is a national user facility operated by Stanford University on behalf of the U.S. Department of Energy, Office of Basic Energy Sciences. The SSRL Structural Molecular Biology Program is supported by the Department of Energy, Office of Biological and Environmental Research, and by the National Institutes of Health, National Center for Research Resources, Biomedical Technology Program. Funding for the MAX-Lab beamline I811 was provided by The Swedish Research Council and The Knut och Alice Wallenbergs Stiftelse, and we are grateful for the additional support from Dr. Stefan Carlson at MAX-Lab beamline I811.

Note Added after ASAP Publication. This paper was published on the Web on April 16, 2010, with the incorrect artwork for Figure 3. The corrected version was reposted on April 20, 2010.

Supporting Information Available: Additional information as noted in the text. This material is available free of charge via the Internet at http://pubs.acs.org.